Ni-Catalyzed Electrochemical C(sp^2)−C(sp^3) Cross-Coupling Reactions

Jian Luo, Bo Hu, Wenda Wu, Maowei Hu, T. Leo Liu*

*Corresponding Author: leo.liu@usu.edu and liutbrss@gmail.com

Department of Chemistry and Biochemistry, Utah State University, Logan, Utah 84322, USA

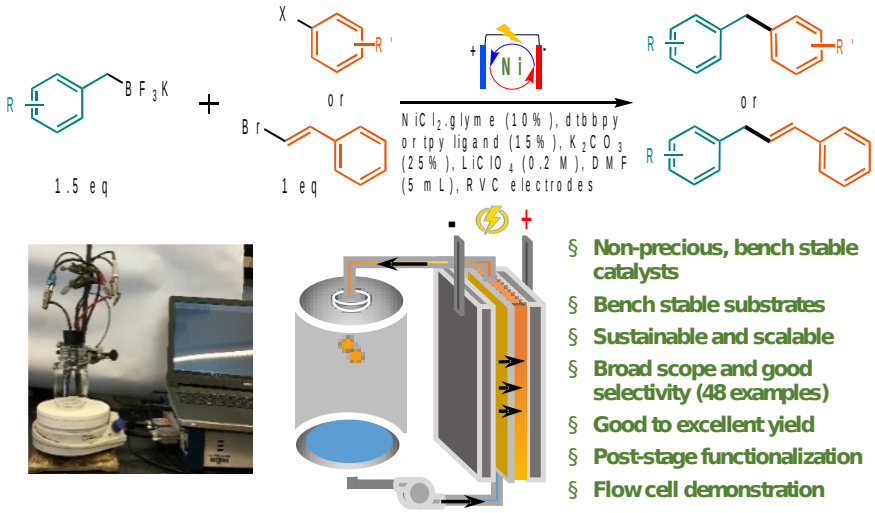

Abstract: Nickel (Ni) catalyzed carbon-carbon (C−C) cross-coupling has been considerably developed in last decades and has demonstrated unique reactivities compared to palladium. However, existing Ni catalyzed cross-coupling reactions, despite success in organic synthesis, are still subject to the use of air-sensitive nucleophiles (i.e. Grignard and organozinc reagents), or catalysts (i.e. Ni^0 pre-catalysts), significantly limiting their academic and industrial adoption. Herein, we report that, through electrochemical voltammetry screening and optimization, the redox neutral C(sp^2)−C(sp^3) cross-coupling can be accomplished in an undivided cell configuration using bench-stable aryl halide or β-bromostyrene (electrophiles) and benzylic trifluoroborate (nucleophiles) reactants, non-precious, stable catalysts consisting of $NiCl_2$•glyme pre-catalyst and polypyridine ligands under ambient conditions. The broad reaction scope and good yields of the Ni-catalyzed electrochemical coupling reaction were confirmed by 48 examples of aryl/β-styrenyl chloride/bromide and benzylic trifluoroborates. Its potential applications were demonstrated by late-stage functionalization of pharmaceuticals and natural amino acid modification. Furthermore, this electrochemical C−C cross-coupling reaction was demonstrated at gram-scale in a flow-cell electrolyzer for practical industrial adoption. Finally, an array of chemical and electrochemical studies mechanistically indicates that electrochemical

C−C cross-coupling reaction proceeds through an unconventional radical trans-metalation mechanism.

In the past half-century, transition metal catalyzed carbon-carbon (C−C) cross-coupling reactions have gained significance advances regarding reaction scopes, selectivity, and catalytic mechanisms, and achieved tremendous success in organic synthesis of pharmaceutical molecules, agrochemicals, and organic materials.[1-3] Catalyzed C−C cross-coupling reactions have historically been dominated by Pd-based catalysts.[4, 5] In addition to replacing the expensive, precious Pd metal, Ni metal is characteristic of more negative 2+/0 and 1+/0 redox potential than $Pd^{2+/0}$ to enable unique oxidative addition reactivities in activating C-X (X = Cl and Br) bonds[6] and has found increasing importance in C-C cross coupling reactions.[7, 8] However, Ni catalyzed C−C cross-coupling reactions are still limited by a number of well-known synthetic limitations. Ni-based Kumda, Negish, and Suzuki, and reductive couplings are practically hampered by the use of either strong nucleophiles, sacrificed reductants, or sensitive Ni^0 pre-catalysts, e.g. widely used $Ni(COD)_2$ (where COD is 1,5-cyclooctodiene) and typically require rigid reaction conditions using inert atmosphere glovebox or Schenk-line techniques. It remains a long-standing challenge to develop Ni-catalyzed cross-coupling reactions using bench stable chemicals and easy-handling conditions for widespread academic and industrial adoption.[8] Efforts have been made to develop well-defined air stable Ni^{II} and Ni^0 pre-catalysts[9-11] and encapsulated Ni^0 pre-catalysts.[12] However, these practices are limited by the pre-formation of Ni pre-catalysts under rigid air-free conditions and the need of special stabilization ligands for most of them.

On the other side, literature has witnessed the powerful applications of electrochemistry in organic synthesis.[13-15] By precisely controlling redox potentials in an electrolyzer cell, substrates or catalysts can be selectively anodically or catholically activated to participate desired reaction sequences.[13-15] Thereby, electrochemical reactions not only migrate the use of reactive (even dangerous and toxic) oxidants and reductants and enable the access of highly reactive catalytic intermediates which are not easily handled in traditional thermal reactions, representing a green, atomically economical synthetic strategy. In spite of being known for many decades, until very recently electrochemical synthesis has aroused recurred attention and is believed to impart

profound impacts on organic syntheis.[13-15] For instance, anodic reactions including alcohol oxidation,[16] C−H functionalization,[17-19] alkene functionalization,[20, 21] cyclization,[22, 23] and C−O[24] and C-N[25, 26] couplings, and cathodic reactions including arene or alkene hydrogenation,[27, 28] and arylboronic acid hydroxylation[29] were demonstrated with good selectivity and yields. We envisioned that the synergic coupling of single electron transfer (SET) anodic oxidation and cathodic reduction process could enable unprecedented electrochemical C−C cross-coupling reactions which hold promise to address the above-mentioned limitations of two-electron redox based traditional Ni-catalyzed thermal coupling reactions. Ni-catalyzed cathodic Heck-type[30] and reductive[31] C−C couplings were recently demonstrated, still requiring the use of a sacrificed anode electrode.

Instead of randomly testing combinations of nucleophiles, electrophiles, and catalysts, we first set out to identify individual anodic and cathodic SET half-cell reactions for the proposed full-cell C−C coupling reactions using the electrochemical cyclic voltammetry (CV) method. For the cathodic half-cell reaction, we aimed to explore for the SET reduction of Ni^{II}-based catalysts to activate aryl and vinyl halide electrophiles by the $Ni^{III/I(II/0)}$redox cycle to achieve R−$Ni^{III(II)}$−X intermediate, which is mechanistically accessible in traditional Ni-based thermal couplings.[6] For the anodic half-reaction, nucleophiles including carboxylic acid[13] and organic trifluoroborate[32] are well documented as carbon radical precursors (R′• in Figure 1) upon SET oxidation. Herein, we chosen potassium butyrate, pivalate, phenylacetate, butyltrifluoroborate and benzyltrifluoroborate as C(sp^3) sources; potassium benzoate, 3-methylcrotonate, and phenyltrifluoroborate as C(sp^2) sources; potassium 2-butynoate as C(sp) source (Figure 2A). The proposed concept is illustrated in Figure 1. In principle, if adopting a $Ni^{III/I}$ redox cycle, a bench stable Ni^{II} precursor can be activated by one electron reduction using a catalytic amount of a redox active nucleophile to access the R−Ni^{III}−X intermediate through oxidative addition. Then after another electron reduction while a R′• radical is generated anodically, the R−Ni^{II}−X intermediate can trap the R′• radical to form a high-valent R−Ni^{III}(X)−R′ intermediate through single-electron transmetallation. Finally, the desired C−C cross-coupling product would be produced accompanying with the regeneration of the Ni^{I} catalyst through a reductive elimination reaction. The designed electrochemical C−C cross coupling reaction is (1) fundamentally attractive as a new means to forge C−C bonds, (2) practically attractive without involving reactive reactants and expensive metals, and (3) atomically economic and environmentally

friendly by avoiding the use of sensitive (even dangerous and toxic) sacrificial chemical reductants or oxidants.

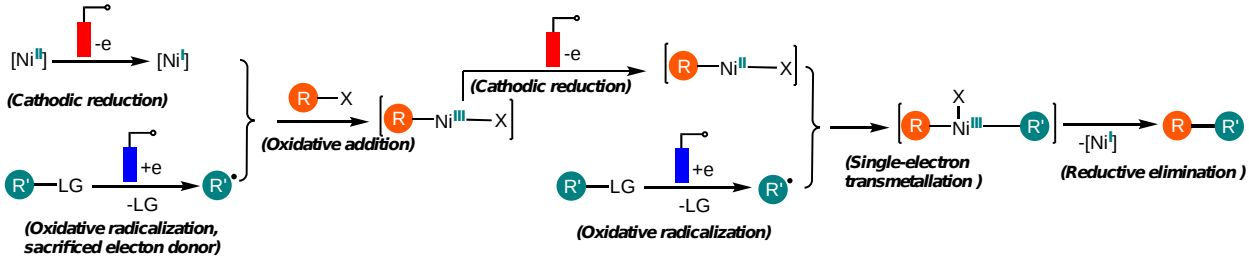

Figure 1. Designed Ni-catalyzed electrochemical C−C cross-coupling reaction. X, halide; LG, leaving group.

Electrochemical screening of the proposed half-cell reactions was conducted through the cyclic voltammetry (CV) method using a three-electrode system. As shown in Figure 2B(i) (gray curve), in the presence of 3 equivalents 2,2'-bipyridine (2,2'-bpy) ligand, $NiCl_2$•glyme displayed a reversible redox signal at $E_{1/2}$ = –1.49 V (vs. $Fc^{+/0}$), which corresponding to the $Ni^{II/I}$ redox couple. Then, 10 equivalents of organic halides (R−X) were added to the electrolyte and CV curves were collected again. Among tested organic halides, $C(sp^2)$ precursors (arly halide and alkenyl bromide) or C(sp) precursors (alkynyl bromide) could be activated by the Ni^{I} intermediate while $C(sp^3)$ precursors were inactive. For example, when methyl 4-bromobenzoate was added (green trace in Figure 2B(i)), the reductive peak current intensity was obviously increased, meanwhile, the return peak disappeared which indicates that an irreversible chemical reaction happened between Ni^{I} species and the aryl halide. The same screening experiments were conducted to the anodic substrates. As shown in Figure 2B(ii), in 0 – 1.25 V (vs. $Fc^{+/0}$) potential range, only potassium benzyltrifluoroborate, phenylacetate, and pivalate displayed remarkable electrochemical reactivity with peak potentials at +0.75 V, +0.94 V, and +1.02 V (vs $Fc^{+/0}$), respectively. Other substrates were electrochemically inert in the scanned potential range. Based on the CV screening results for both cathodic and anodic substrates, $C(sp^2)$ precursors (aryl halide and alkenyl bromide) or C(sp) precursors (alkynyl bromide) and $C(sp^3)$ sources (potassium benzyltrifluoroborate, phenylacetate, and pivalate) were possible combinations for electrochemical $C(sp^2)$−$C(sp^3)$ or C(sp)−$C(sp^3)$ cross-coupling reactions.

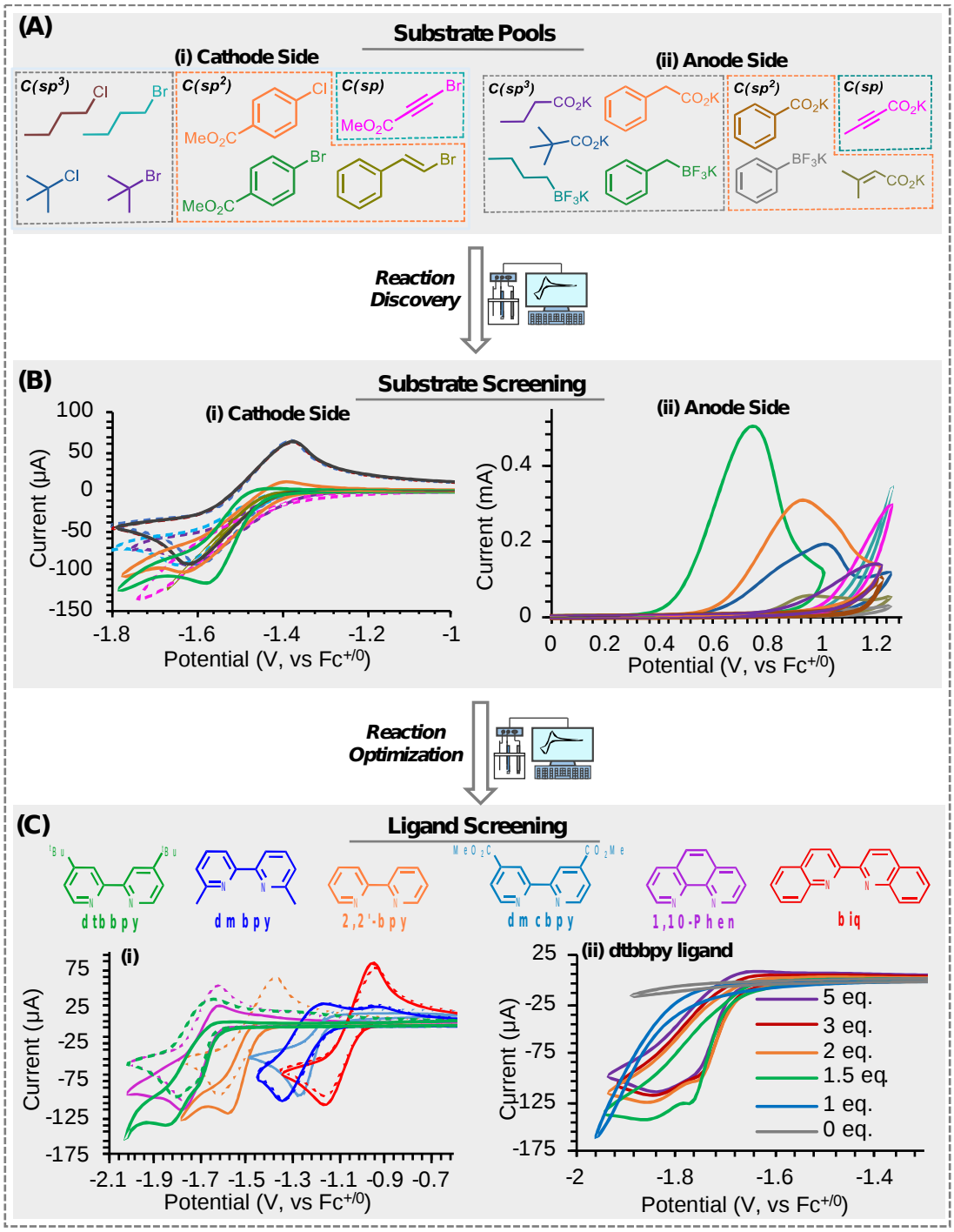

Figure 2. Electrochemical voltammetry screening of cathodic and anodic half-reactions. (**A**) Selected substrate pools. (**B**) CV screening to identify reactive substrates of cathodic (i) and anodic (ii) half-reactions. The CV curves were recorded with 5 mM $NiCl_2$.glyme, 15 mM 2,2'-bpy, and 50 mM organic halides for the cathode side screening, 0.1 M potassium trifluoroborates or carboxylates for the anode side screening. DMF solvent, 0.2 M $LiClO_4$ supporting electrolyte,

GC working electrode, 100 mV/s scan rate, room temperature. (**C**) CV screening of the ligand (i) and Ni/ligand ratio (ii) to optimize the cathodic half-reaction. The ligand screening curves were recorded with 5 mM $NiCl_2$.glyme and 15 mM ligand in the presence (dash line) and absence (solid line) of 50 mM methyl 4-bromobenzoate. The Ni/ligand ratio screening curves were recorded with 5 mM $NiCl_2$.glyme and 50 mM methyl 4-bromobenzoate by adding various ratio of dtbbpy ligand.

We then optimized the $NiCl_2$•glyme/polypyridine catalyst system using cyclic voltammetry with methyl 4-bromobenzoate as a model electrophile. As shown in Figure 2C(i), seven different polypyridine ligands including 4,4'-di-tert-butyl-2,2'-bipyridyl (dtbbpy), 6,6'-dimethyl-2,2'-bipyridyl (dmbpy), 2,2'-bpy, dimethyl 2,2'-bipyridine-4,4'-dicarboxylate (dmcbpy), 1,10-phenanthroline (1,10-Phen), and 2,2'-biquinoline (biq) were screened to identify the most suitable ligand for the Ni-catalyst. Among all the ligands, dtbbpy prompted the strongest current intensity increase (green curve), indicating that $Ni^{I}(dtbbpy)^{+}$ is the most reactive species to oxidative addition of the C–Br bond of methyl 4-bromobenzoate. Besides 2,2'-bpy and dtbbpy, 1,10-Phen also aroused strong current response (purple curve) and thus can also be a suitable ligand. We further investigated the effect of Ni/ligand ratio on the reactivity of the Ni-catalyst. The CV curves of $NiCl_2$•glyme with addition of various ratio of dtbbpy ligand showed continuous change (Figure S5). In the absence of dtbbpy ligand, no reversible redox signal was observed. When 1 ~ 3 equivalents of dtbbpy ligand was added, there were two set of quasi-reversible redox signals. Further increase the ligand ratio to 5 equivalents, the redox signals overlapped to one set of fully reversible redox signal. It indicates that there is an equilibrium for Ni^{II} complexes in the solution: $Ni^{II} \leftrightarrow Ni^{II}(dtbbpy) \leftrightarrow Ni^{II}(dtbbpy)_2 \leftrightarrow Ni^{II}(dtbbpy)_3$, which is consistent with a previous UV-vis study. In the presence of methyl 4-bromobenzoate substrate, the addition of 1.5 equivalent of dtbbpy ligand (Figure 2C(ii), green curve) yielded the highest cathodic current. Adding more ligand (2 – 5 equivalents), the reductive peak current intensity slightly decreased and the return peak gradually showed up, which is most likely due to the decreased reactivity of Ni-catalyst after coordination to multiple dtbbpy ligands ($Ni(dtbbpy)_2$ and $Ni(dtbbpy)_3$).

Encouraged by the positive observations in the electrochemical voltammetry studies, we proceeded to test the $C(sp^2)$–$C(sp^3)$ cross-coupling full-reaction by combining the oxidative

radicalization of benzylic trifluoroborates and Ni-catalyzed C−X activation of aryl halides in an undivided cell. A starting electrolysis system consisting of $NiCl_2$•glyme catalyst, dtbbpy ligand, and $LiClO_4$ supporting electrolyte confirmed the cross-coupling of methyl 4-bromobenzoate and potassium benzyltrifluoroborate in 47% yield (produce methyl 4-benzylbenzoate, **1**) after galvanostatic electrolysis at 3.0 mA for 28 h. Dimethyl 4,4'-biphenyldicarboxylate (**1'**) from the homo-coupling of methyl 4-bromobenzoate was isolated as the main by-product in 38% yield. To further improve the reaction yield, a number of supporting electrolytes ($TBAPF_6$, KPF_6, and NaBF4) and salt additives (K_2CO_3, Na_2CO_3, and KOAc) were tested to optimize the reaction efficiency (Table S1). It was found that the yield for **1** was further improved to 93% using K_2CO_3 additive. The essentiality of $NiCl_2$•glyme catalyst, dtbbpy ligand, and electrolysis was determined by control experiments (Table S1, SI). In addition, both reaction selectivity and rate were largely affected by current intensity. Poorer selectivity was obtained under a higher or lower current intensity (64% under 1.0 mA, 77% under 5.0 mA current). Under 1.0 mA current electrolysis, the reaction was significantly decelerated as a reaction time of 48 h needs to fully convert the substrate. Other solvents, such as THF, MeCN, CH_2Cl_2, MeOH, and DMSO were not effective to this reaction (only 0 – 15% yield was observed, Table S2, SI). Moreover, similar as under thermal reaction conditions,[16] the reactivity and selectivity of this reaction is highly sensitive to the ligand structure (Table S3, SI). In particular, dtbbpy and 2,2'-bpy ligands exhibited the best efficiencies with isolated yields of 93% and 87%, respectively. 1,10-Phen and tridentate terpyridine (tpy) ligands gave moderate yields of 67% and 73%, respectively. It is noteworthy that the best selectivity between cross-coupling product **1** and homo-coupling product **1'** (96:4) was obtained by using tpy ligand, which tends to suppress the homo-coupling of strong electrophiles. However, other ligands (dmbpy, dmcbpy, and biq) were not effective.

After establishing optimal reaction conditions for the Ni-catalyzed electrochemical $C(sp^2)$–$C(sp^3)$ cross-coupling reaction, we next tested the reaction scope on both aryl halide and benzylic trifluoroborate. As shown in Figure 3, a wide range of aryl chlorides including both electron-rich and electron-deficient arenes were suitable to this Ni-catalyzed electrosynthesis system (**1** to **5**). The electron-deficient aryl chlorides (**1** to **3**, 74% to 86% yield) delivered better yield than the electron-rich ones (**4** and **5**, 46% and 31% yield). It is probably due to the low activity of electron-rich aryl chloride substrates with the Ni^I intermediate. Aryl bromides displayed better efficiencies than the corresponding aryl chlorides, as **1** to **5** were isolated in 77% to 93% yield by

using aryl bromide substrates. The reaction exhibited comparable efficiency upon scale-up, for example, 89% yield was obtained on a 2.5 mmol scale reaction of **1** (0.5 g). The substituent position of aryl bromide displayed moderate effect to the reaction efficiency, as the para-, meta- and ortho-substituted methyl bromobenzoate delivered 93%, 71%, and 89% yield (**1**, **6** and **7**), respectively. Aryl bromides with functional groups as diverse as ester (**1**, **6**, **7**, and **10**), ketone (**2**), fluoride (**3**), methoxy group (**9** and **10**), amide (**14** and **15**), aldehyde (**11**), nitrile (**12**) and alkenyl (**19**) were effective in this reaction. Substrates possessing strongly electron-donating substituents such as ^{t}Bu and methoxy groups could also provide moderate to good yield (72% for **8** and 53% for **9**). It is interesting that for the substrates possessing strong electron-withdrawing substituents such as aldehyde, acetyl, and cyano groups, best results were obtained by using 2,2'-bpy ligand (83% and 91% yield for **2** from chloride and bromide, respectively, 82% yield for **11**, and 74% yield for **12**). Furthermore, in the case of 4-bromo(trifluoromethyl)benzene, homo-coupling product, 4,4'-bis-(trifluoromethyl)biphenyl (**13'**), was obtained as the only product when using dtbbpy and 2'2-bpy ligands. Interestingly, 21% yield of cross-coupling product **13** was obtained by using the tpy ligand.

In addition to examine the substituent positions and functional groups of the aryl halide substrates, we also investigated the tolerance of this electrosynthesis system to common protecting groups which are widely used in organic synthesis, such as amide, tert-butyloxycarbonyl (Boc), benzyl ether (BnO), and acetal. All of these protecting groups were well tolerated, as evidenced by good isolation yield of **14** to **18** (67% to 86% yield). The π-conjugation extended aryl bromide substrates including 4-bromophenylethene, 3-bromofluorene, and 2-bromonaphthalene also smoothly proceeded this cross-coupling reaction with moderate to good yield (**19** to **21**, 43% to 84% yield). Moreover, a variety of aryl bromides consisting nitrogen-containing heterocyclic including 6-bromoquinoline, 6-bromoisoquinoline, and Boc protected 6-bromotetrahydroisoquinoline, and 5-bromoindole, which are prevalent building blocks in bio-active molecules, delivered moderate to good yield (**22** to **25**, 52% to 81% yield).

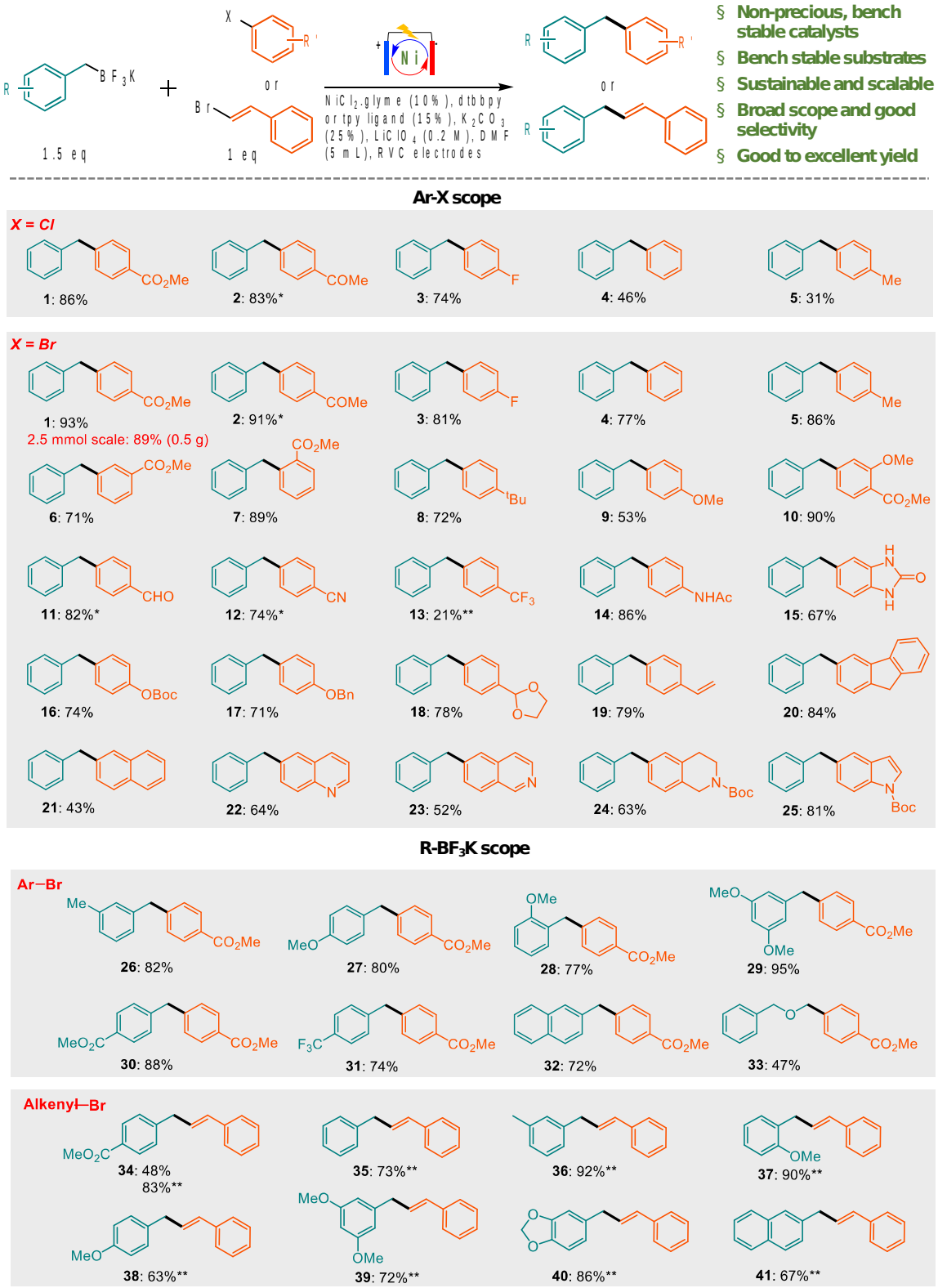

Figure 3. Substrate scope of the Ni-catalyzed electrochemical C(sp^2)–C(sp^3) cross-coupling reaction. Yields refer to isolated yields of products after chromatography on silica gel. Standard

conditions: aryl halide or β-bromostyrene substrate (0.5 mmol), trifluoroborate substrate (0.75 mmol), $NiCl_2$.glyme (50 μmol), dtbbpy ligand (75 μmol), K_2CO_3 (1.25 mmol), $LiClO_4$ (0.2 M), DMF (5 mL), RVC as anode and cathode, 3 mA current electrolysis under Ar at room temperature for 20 – 36 h. *75 μmol 2,2'-bppy as ligand. **50 μmol tpy as ligand. In case of **13**, an inseparable mixture of **13** and **13'** was obtained, 41% purity.

The substrate scope of benzylic trifluoroborate salts was also investigated. As shown in Figure 3, both electron-rich and electron-deficient benzylic trifluoroborates were approved efficient carbon radial precursors in this cross-coupling reaction (**26** to **31**, 74% to 95% yield). Functional groups, including esters, methoxy group, and trifluoromethyl group were tolerant to this Ni-catalyzed electrosynthesis. The substituent positions displayed negligible effects to the reaction efficiency, as comparable yield was obtained for the para-, meta-, and ortho-substituted benzylic trifluoroborates (**26** to **28**, 77% to 82% yield). In the presence of two strong electron-donating methoxy (MeO-) groups, the highest yield, 95%, was gained for **29,** which is interpreted as the favorable oxidation kinetics of the corresponding trifluoroborate substrate. The π-conjugation extended naphthalen-2-ylmethyl trifluoroborate is also highly productive in this electrochemical $C(sp^2)–C(sp^3)$ cross-coupling reaction, as 72% yield was obtained for **32**. Beside the benzylic trifluoroborates, ((benzyloxy)methyl)trifluoroborate also manifested reasonable reactivity in this reaction with a yield of 47% (**33**).

In the CV screening studies (Figure 2B), some other substrates also showed reactivity in the anodic half-reaction. For example, β-bromostyrene and methyl 3-bromopropiolate showed reactivity in the anodic half-cell reaction (Figure S4, SI). When β-bromostyrene was used as an electrophile to react with potassium trifluoro(4-(methoxycarbonyl)benzyl)borate, 48% yield of the Heck-like $C(sp^2)–C(sp^3)$ cross-coupling product **34** and 47% yield of the homo-coupling product **34'** were obtained by using dtbbpy as ligand. To suppress the homo-coupling product, best yield and selectivity for the cross-coupling product **34** was obtained in the presence of tpy ligand (83% yield, 90% selectivity) (Table S4, SI). As shown in Figure 3, both electron-rich and electron-deficient benzylic trifluoroborates were efficient in this cross-coupling reaction (**34** to **40**, 63% to 92% yield). Functional groups including esters, methoxy group, and benzodioxol group were tolerant in this Ni-catalyzed electrochemical reaction. The π-conjugation extended naphthalen-2-ylmethyl trifluoroborate also provided good reactivity in this reaction, as 67% yield

was obtained for **41**. However, other anodic nucleophiles (3-bromopropiolate, phenylacetic acid, potassium pivalate, and potassium phenyltrifluoroborate) didn't provide satisfactory results (see Figure S7 and the SI for more discussions).

To demonstrate potential applications of this Ni-catalyzed electrochemical C(sp^2)–C(sp^3) cross-coupling reaction, we utilized it in late-stage functionalization of pharmaceuticals which is a popular way for fast discovery of new drag candidates. Fenofibrate is a pharmaceutical molecule of the fibrate class and used to treat abnormal blood lipid levels. As shown in Figure 4A, using our electrosynthesis method, Fenofibrate was successfully converted to a series of brand-new compounds (**42** to **46**, 41% to 86% yield) in up to 2.5 mmol (0.93 g) scale form a regular vial electrolyzer cell. To testify the potential industrial adoption of this innovative electrochemical C−C cross-coupling reaction, the synthesis of **46** was further scaled up to 8 mmol (3.2 g) using a flow-cell electrolyzer (Figure 4D and 4E). Under the flow-cell condition, an even better reaction efficiency (84% yield) was obtained compared to the vial reaction (81% yield). Another new Clofibrate derivative (a lipid-lowering agent) was synthesized using this electrochemical approach (**47**, 63% yield) (Figure 4B). Furthermore, the electrochemical C−C cross-coupling reaction was also effective in modification of brominated natural amino acid, e.g. phenylalanine, (Figure 4C) (**48**, 83% yield).

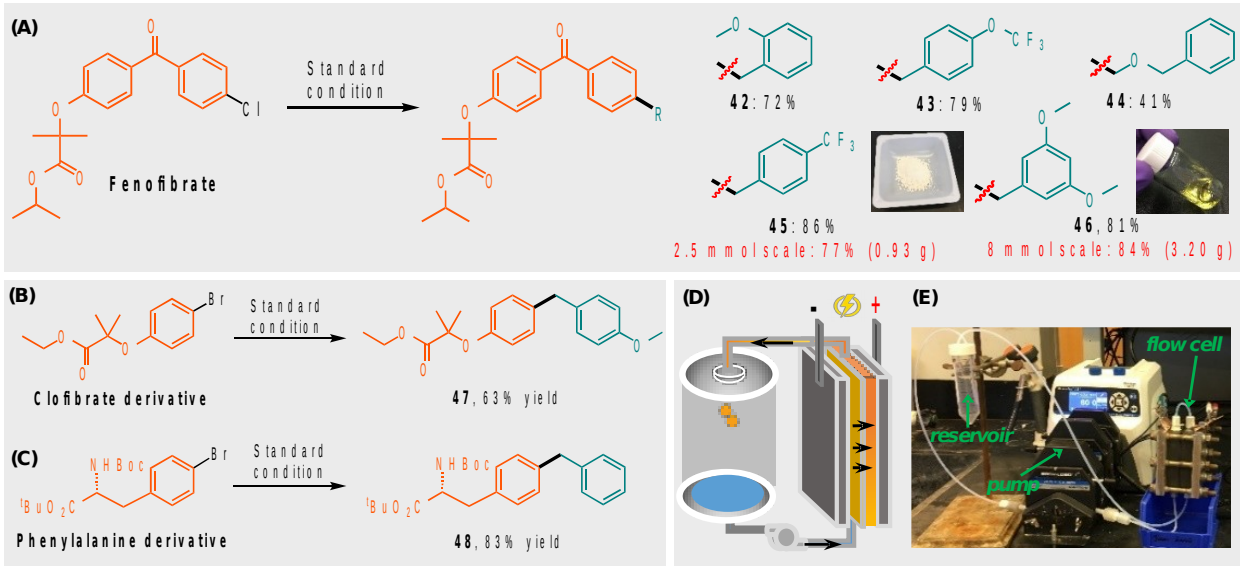

Figure 4. Applications of the Ni-catalyzed electrochemical C(sp^2)–C(sp^3) cross-coupling reaction. Late-stage functionalization of Fenofibrate (**A**), Clofibrate derivative (**B**), and modification of brominated phenylalanine (**C**). (**D**) schematic drawing and (E) experimental

setup of the electrosynthesis flow-cell. Yields refer to isolated yields of products after chromatography on silica gel.

To gain mechanism understandings of this Ni-catalyzed electrochemical C(sp^2)–C(sp^3) cross-coupling reaction, radical-trapping experiment was conducted for the anodic half-reaction. As shown in Figure 5A, controlled potential electrolysis (at 1.2 V, vs. $Fc^{+/0}$) of the potassium trifluoro(4-(methoxycarbonyl)benzyl)borate and 2,2,6,6-tetramethyl-1-piperidinyloxy (TEMPO) in a divided-cell produced radical coupling product **49** with 86% isolated yield, which confirms the formation of 4-(methoxycarbonyl)benzyl free radical in the anodic oxidation process. In aadition, plots of overpotential over the logarithm of kinetic current and the corresponding fitted Tafel plots were constructed to determine charge transfer rate constants (k^0) of potassium benzyltrifluoroborate and cesium phenylacetate in the anodic oxidation process (Figure 5B and see the SI for detail). k^0 of potassium benzyltrifluoroborate and cesium phenylacetate were calculated as 5.56 x 10^{-5} cm/s and 1.39 x 10^{-5} cm/s, respectively. The higher charge transfer rate constant of potassium benzyltrifluoroborate indicates faster electrochemical reactivity to generate carbon radicals than cesium phenylacetate, which is consistent with the better efficiency of potassium benzyltrifluoroborate in the cross-coupling reaction than cesium phenylacetate. It is believed that the quick formation of the carbon radical is critical to trap the R-Ni^{II}-X intermediate, otherwise the R-Ni^{II}-X intermediate can promote the homo-coupling side reaction.

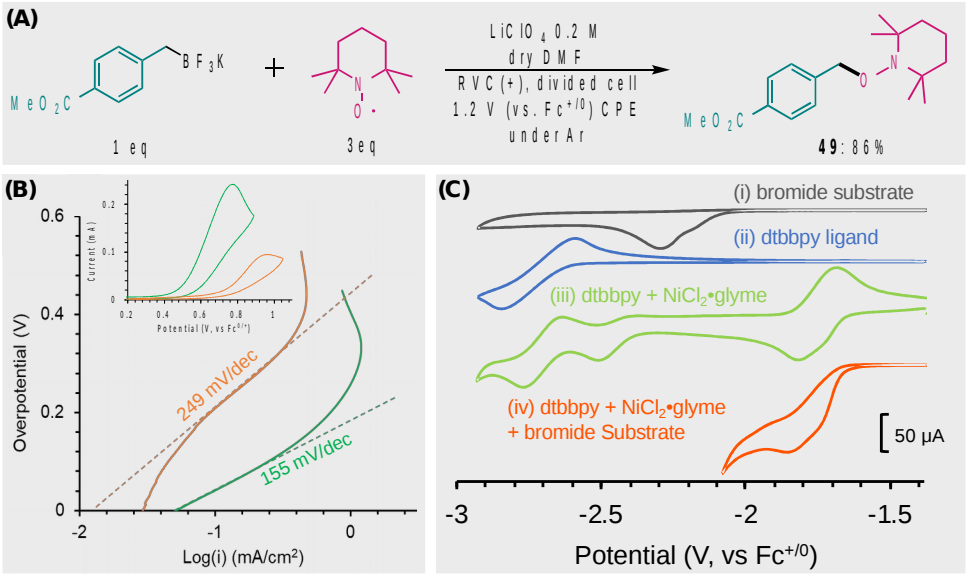

Figure 5. Reaction mechanism studies of the Ni-catalyzed electrosynthesis system. (A) Carbon free radical trapping reaction. (**B**) Plots of overpotential over the logarithm of kinetic current and the fitted Tafel plots of phenyl trifluoroborate (green) and cesium phenylacetate (orange). Inset: CV curves of potassium phenyl trifluoroborate (green) and cesium phenylacetate (orange); conditions: 10 mM in DMF, $LiClO_4$ (0.2 M) supporting electrolyte, GC working electrode, and 100 mV/s scan rate. **(C)** CV curves of 50 mM methyl 4-bromobenzoate (gray), 15 mM dtbbpy ligand (blue), 5 mM $NiCl_2$•glyme + 25 mM dtbbpy (green), and 5 mM $NiCl_2$•glyme + 15 mM dtbbpy + 50 mM methyl 4-bromobenzoate (orange) in DMF with 0.2 M $LiClO_4$ supporting electrolyte.

Additional CV studies were conducted to gain additional mechanistic insights for the cathodic process. As shown in Figure 5B, methyl 4-bromobenzoate substrate displayed irreversible redox signal with onset potential at -2.05 V (vs $Fc^{+/0}$) and dtbbpy ligand delivered reversible redox signal with $E_{1/2}$ = -2.70 V (vs. $Fc^{+/0}$), respectively. The mixture of $NiCl_2$•glyme and dtbbpy ligand delivered three redox peaks at $E_{1/2}$ = -1.74 V, -2.44 V, and -2.70 V (vs. $Fc^{+/0}$), which corresponding to $Ni^{II/I}$, $Ni^{I/0}$ redox couples, and the free ligand. When the methyl 4-bromobenzoate substrate was added, significant increase of reductive current and disappearing of the return peak was observed for the $Ni^{II/I}$ redox couples. It indicated that the Ni^{I} is the reactive species for oxidative addition to aryl halide. In addition, CV curves of the reaction mixture displayed -1.60 V and 0.33 V (vs. $Fc^{+/0}$) onset potentials for cathodic and anodic half-reactions, respectively (Figure S8). The potential of cathode kept between -1.7 and -1.9 V (vs. $Fc^{+/0}$) during the reaction (Figure S9), which indicates the $Ni^{I/0}$ redox couple is not involved in the cathodic process.

Based on the chemical and electrochemical studies, a possible reaction mechanism for this Ni-catalyzed electrochemical $C(sp^2)–C(sp^3)$ cross-coupling is proposed and illustrated in Figure 6. The reaction is initiated by the electrochemical reduction of Ni^{II} catalyst **A** to Ni^{I} species **B**, the latter further oxidative addition to aryl halide substrate **C** to generate an $Ar–Ni^{III}$ complex **D**. **D** is subsequently electrochemically reduced to $Ar–Ni^{II}$ species **E**. Simultaneously, a benzylic carbon free radical **G** generated through oxidative degradation of benzylic trifluoroborate or phenylacetate substrate **F** in the anode side is captured by **E** to form a high-valent $Ar–Ni^{III}–Bn$

species **H**. Then, **H** undergoes reductive elimination to produce the cross-coupling product **I** and recover the Ni^{I} catalyst **B**.

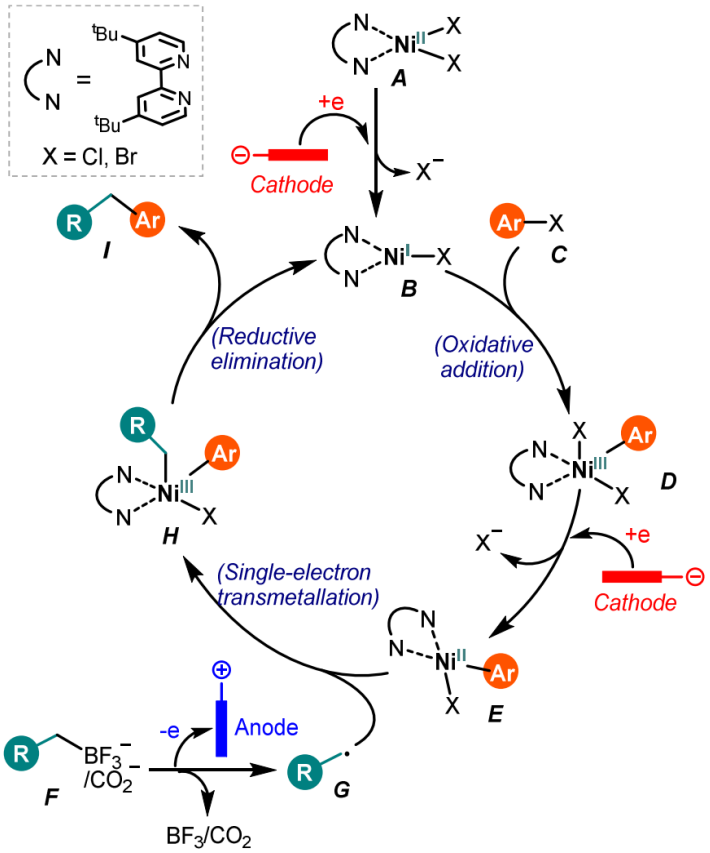

Figure 6. Proposed reaction mechanism for the Ni-catalyzed electrochemical C(sp^2)–C(sp^3) cross-coupling reaction.

In summary, a Ni-catalyzed electrochemical cross-coupling methodology was developed to forge the C(sp^2)–C(sp^3) bond with broad substrate scope, excellent functional group tolerance, selectivity, and good yield. In addition, the cyclic voltammetry proved an effective and efficient way for the discovery, optimization, and mechanistic understanding of anodic and cathodic half-reactions and can be used as a go-to method for developing other useful electrosynthesis methodologies. Compared to traditional thermal Ni catalyzed cross-coupling reactions, the present electrochemical approach is advantageous as all reactants and catalysts are bench stable without using reactive oxidants/reductants and complex inert atmosphere techniques. As exemplified in gram-scale synthesis in flow-cell and late-stage functionalization of

pharmaceuticals, this electrochemical C−C coupling methodology are expected to be widely applied to the construction of $C(sp^2)–C(sp^3)$ bonds in developing pharmaceutical molecules, agrochemicals, and organic materials. The Ni-catalyzed electrochemical C-C cross reactions can be further advanced for broader substrates and extended to other types of coupling reactions. Moreover, the present new C-C bond formation paradigm (and also extended reactions) can offer rich opportunities to pursue fundamental mechanistic studies and thus lead to the discovery of new catalytic knowledge at the interface of synthetic chemistry and electrochemistry.

References:

[1] A. De Meijere, F. Diederich, *Metal-Catalyzed Cross-Coupling Reactions*, 2 ed., Wiley-VCH: Weinheim, Germany, **2004**.
[2] E.-i. Negishi, *Angew. Chem. Int. Ed.* **2011**, *50*, 6738-6764.
[3] A. Suzuki, *Angew. Chem. Int. Ed.* **2011**, *50*, 6722-6737.
[4] X.-F. Wu, P. Anbarasan, H. Neumann, M. Beller, *Angew. Chem. Int. Ed.* **2010**, *49*, 9047-9050.
[5] C. C. C. Johansson Seechurn, M. O. Kitching, T. J. Colacot, V. Snieckus, *Angew. Chem. Int. Ed.* **2012**, *51*, 5062-5085.
[6] J. B. Diccianni, T. Diao, *Trends in Chemistry* **2019**.
[7] R. Jana, T. P. Pathak, M. S. Sigman, *Chem. Rev.* **2011**, *111*, 1417-1492.
[8] S. Z. Tasker, E. A. Standley, T. F. Jamison, *Nature* **2014**, *509*, 299.
[9] E. A. Standley, T. F. Jamison, *J. Am. Chem. Soc.* **2013**, *135*, 1585-1592.
[10] J. D. Shields, E. E. Gray, A. G. Doyle, *Org. Lett.* **2015**, *17*, 2166-2169.
[11] L. Nattmann, R. Saeb, N. Nöthling, J. Cornella, *Nature Catalysis* **2019**.
[12] J. E. Dander, N. A. Weires, N. K. Garg, *Org. Lett.* **2016**, *18*, 3934-3936.
[13] K. D. Moeller, *Tetrahedron* **2000**, *56*, 9527-9554.
[14] M. Yan, Y. Kawamata, P. S. Baran, *Chem. Rev.* **2017**, *117*, 13230-13319.
[15] A. Wiebe, T. Gieshoff, S. Möhle, E. Rodrigo, M. Zirbes, S. R. Waldvogel, *Angew. Chem. Int. Ed.* **2018**, *57*, 5594-5619.
[16] A. Badalyan, S. S. Stahl, *Nature* **2016**, *535*, 406-410.
[17] E. J. Horn, B. R. Rosen, Y. Chen, J. Z. Tang, K. Chen, M. D. Eastgate, P. S. Baran, *Nature* **2016**, *533*, 77-81.
[18] F. Wang, M. Rafiee, S. S. Stahl, *Angew. Chem.* **2018**, *130*, 6796-6800.
[19] S. Tang, L. Zeng, A. Lei, *J. Am. Chem. Soc.* **2018**, *140*, 13128-13135.
[20] N. Fu, G. S. Sauer, A. Saha, A. Loo, S. Lin, *Science* **2017**, *357*, 575-579.
[21] K.-Y. Ye, G. Pombar, N. Fu, G. S. Sauer, I. Keresztes, S. Lin, *J. Am. Chem. Soc.* **2018**, *140*, 2438-2441.
[22] Z.-W. Hou, Z.-Y. Mao, H.-B. Zhao, Y. Y. Melcamu, X. Lu, J. Song, H.-C. Xu, *Angew. Chem. Int. Ed.* **2016**, *55*, 9168-9172.
[23] Z.-W. Hou, Z.-Y. Mao, Y. Y. Melcamu, X. Lu, H.-C. Xu, *Angew. Chem. Int. Ed.* **2018**, *57*, 1636-1639.
[24] J. Xiang, M. Shang, Y. Kawamata, H. Lundberg, S. H. Reisberg, M. Chen, P. Mykhailiuk, G. Beutner, M. R. Collins, A. Davies, M. Del Bel, G. M. Gallego, J. E. Spangler, J. Starr, S. Yang, D. G. Blackmond, P. S. Baran, *Nature* **2019**, *573*, 398-402.

[25] Y. Kawamata, J. C. Vantourout, D. P. Hickey, P. Bai, L. Chen, Q. Hou, W. Qiao, K. Barman, M. A. Edwards, A. F. Garrido-Castro, J. N. deGruyter, H. Nakamura, K. Knouse, C. Qin, K. J. Clay, D. Bao, C. Li, J. T. Starr, C. Garcia-Irizarry, N. Sach, H. S. White, M. Neurock, S. D. Minteer, P. S. Baran, *J. Am. Chem. Soc.* **2019**, *141*, 6392-6402.
[26] X. Yi, X. Hu, *Angew. Chem. Int. Ed.* **2019**, *58*, 4700-4704.
[27] R. S. Sherbo, R. S. Delima, V. A. Chiykowski, B. P. MacLeod, C. P. Berlinguette, *Nature Catalysis* **2018**, *1*, 501-507.
[28] B. K. Peters, K. X. Rodriguez, S. H. Reisberg, S. B. Beil, D. P. Hickey, Y. Kawamata, M. Collins, J. Starr, L. Chen, S. Udyavara, K. Klunder, T. J. Gorey, S. L. Anderson, M. Neurock, S. D. Minteer, P. S. Baran, *Science* **2019**, *363*, 838-845.
[29] J. Luo, B. Hu, A. Sam, T. L. Liu, *Org. Lett.* **2018**, *20*, 361-364.
[30] B. R. Walker, C. S. Sevov, *ACS Catal.* **2019**, *9*, 7197-7203.
[31] T. J. DeLano, S. E. Reisman, *ACS Catal.* **2019**, 6751-6754.
[32] J. Suzuki, M. Tanigawa, S. Inagi, T. Fuchigami, *ChemElectroChem* **2016**, *3*, 2078-2083.